

Limited Communication Stabilization of Multi-Agent Systems to Synchronized and Balanced Phase Arrangements at Desired Angular Frequency

Anoop Jain and Debasish Ghose

Abstract—This paper considers circular motion of multi-agent systems in which all the agents are required to traverse different circles or a common circle at a desired angular frequency. It is required to achieve these collective motions with the heading angles of the agents synchronized or balanced. In synchronization, the agents and their centroid have a common velocity direction, while in balancing, the movement of agents causes the location of the centroid to become stationary. It is assumed that the agents are subjected to limited communication constraints, and exchange relative information according to a time-invariant undirected graph. The feedback control laws to achieve these collective motions are obtained by using Lyapunov theory and LaSalle's invariance principle. Simulations are given to illustrate the theoretical findings.

Index Terms—Synchronization, balancing, multi-agent systems, desired angular frequency, limited communication.

I. INTRODUCTION

There are various engineering applications such as tracking, surveillance, reconnaissance, environmental monitoring, searching, sensing and data collection, where it is required for the multi-agent system to perform a particular collective motion. A multi-agent system might comprise ground vehicles, air vehicles, underwater vehicles or a combination of these. Motivated by these applications, the collective motion where all the agents traverse *i)* different circles, or *ii)* a common circle at the prescribed angular frequency along with their heading angles in synchronized or in balanced formation, are considered in this paper. Synchronization refers to the situation when all the agents, at all times, move in a common direction. A complementary notion of synchronization is balancing, in which all the agents move in such a way that their centroid, which is the average position of all the agents, remains fixed. It is evident in synchronized formation that agents and their centroid move in the same direction. Note that, in this paper, “collective motion” and “formation” are used interchangeably.

The main objective of this paper is to stabilize these collective motions under the assumptions that the agents are initially performing circular motion at different angular frequencies, and the communication among them is restricted in the sense that each agent exchanges information with only a limited number of neighbors. It is further assumed that this interaction topology among agents is time-invariant and undirected.

A. Jain is a graduate student at the Guidance, Control and Decision System Laboratory (GCDSL) in the Department of Aerospace Engineering, Indian Institute of Science, Bangalore, India (email: anoopj@aero.iisc.ernet.in).

D. Ghose is a Professor at the Guidance, Control and Decision System Laboratory (GCDSL) in the Department of Aerospace Engineering, Indian Institute of Science, Bangalore, India (email: dghose@aero.iisc.ernet.in).

This work is partially supported by Asian Office of Aerospace Research and Development (AOARD).

In this paper, we consider identical agents moving in a plane at constant unit speed with second order rotational dynamics. The dynamics of each agent is represented by a state vector, which includes the position, heading angle and angular frequency of each agent as its elements. The desired radius of the collective circular motion is also achieved by controlling the angular frequency of each agent since radius of rotation = angular frequency⁻¹ for an agent circling at unit linear speed.

The present work is inspired by the problems addressed in [1], [2] and [3]. In [1] and [2], various synchronized and balanced formations of a group of agents are obtained under the assumption of all-to-all and limited communication constraints, respectively. In these papers, it is considered that the angular frequency of initial rotations of all the agents is the same and remains constant at all times. In a general scenario, it is more common that the agents are initially revolving around different circles at different angular frequencies. This is the scenario addressed in this paper. In a similar context, the authors in [3], by assuming an all-to-all coupling among agents, present a Lyapunov based approach to stabilize their synchronized and balanced formations at a desired angular frequency. However, unlike [3], in this paper, the various collective motions in synchronized and balanced formations at a desired angular frequency, are obtained by assuming a limited communication topology in which the associated communication graph among agents is time-invariant and undirected. Some related work, but with all-to-all communication, has been presented in [4]. In [5], the idea of heterogeneous controller gains is introduced for an all-to-all coupled multi-agent system, and it is shown that, by selecting suitable controller gains, synchronized and balanced formations can be controlled significantly to obtain not only a desired direction of motion but also a desired location of the centroid. These results are further extended in [6] for the synchronized formation. In [7], the problem of a formation of agents, assumed to be moving in a controllable force field, is studied to achieve a desired stationary or moving collective centroid. Unlike [5]–[7], in this paper, limited communication constraints are taken in to account to achieve the desired synchronized and balanced formations without using heterogeneous controller gains and external force field.

In recent years, stabilization of collective motion of a multi-agent system on a circle is widely studied. In [8], control laws are proposed to stabilize collective circular motion of nonholonomic vehicles around a virtual reference beacon, which is either stationary or moving. Various synchronized and balanced circular formations of all-to-all coupled unicycle type vehicles, with nonidentical and fixed forward velocities, are discussed in [9]. In [10], control algorithms are proposed to

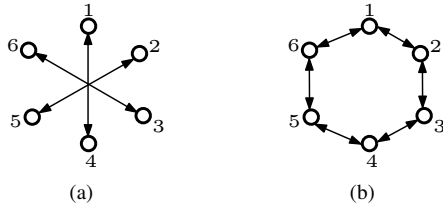


Fig. 1. Undirected circulant graphs for $N=6$. Both (a) and (b) are circulant graphs but only (b) is connected.

stabilize the collective motion of multi-agent systems around a circular orbit, which has a fixed radius and time-varying center. The stabilization of multi-agent system is further discussed in [11] to achieve a circular orbit of a fixed center and time-varying radius. An extension of these results is given in [12], where a new framework based on affine transformations is discussed to achieve more complex time-varying formations. Chen and Zhang [13] propose a decentralized control algorithm for a group of nonholonomic vehicles to stabilize their collective motion, in which the vehicles are evenly distributed over the circle, and have the same rotational radius. The latter assumption is relaxed in [14], where the agents perform a circular motion around a common center, but with different radii. Also, in [14], heterogeneity is assumed in the angular frequencies, however, the forward speed is used as control input. Unlike [10]–[14], in this paper, synchronization and balanced formations of the agents, under limited communication constraint, are ensured around the desired circular orbits. The stabilization of circular motion of a multi-vehicle system under cyclic pursuit is given in the seminal paper [15]. In [16], stabilization of splay formation, characterized by uniform rotation of N evenly spaced agents around a common circle of prescribed radius, is discussed under all-to-all communication scenario. The collective motion of a group of agents, in the symmetric patterns of their phases about a unit circle, is investigated in [17] for a ring-like coupled network in which each agent communicates with exactly two other agents. However, unlike [17], in this paper, the communication topology is relaxed, and deals with connected graphs. Rendezvous problems for completely controllable unicycle-type vehicles, based on limited information, are studied in [18] and [19].

The rest of the paper is organized as follows. In Section II, we describe the system model and problem formulation. In Section III, control laws are proposed to stabilize collective motion of agents on different circles at desired angular frequency with their phase arrangement either in synchronized or in balanced states. The control laws to stabilize collective motion of agents on a common circle of desired radius as well as center with their phase arrangement, again either in synchronized or in balanced states, is proposed in Section IV. The control law to stabilize different symmetric balanced patterns is proposed in Section V. In Section VI, we combine the results of the previous sections and propose control algorithms to stabilize symmetric synchronized and balanced formations suitable for mobile sensor network applications. Finally, Section VII concludes the paper.

II. SYSTEM DESCRIPTION AND PROBLEM STATEMENT

A. Agent Model

Similar to [3], the collective dynamics of N identical agents, moving in a planar space, each assumed to have unit mass and unit speed, is represented as

$$\dot{r}_k = e^{i\theta_k}, \quad \dot{\theta}_k = \omega_k, \quad \dot{\omega}_k = u_k, \quad k = 1, \dots, N. \quad (1)$$

Here, complex notations are used to describe the position and velocity of each agent. For $k = 1, \dots, N$, the position of the k^{th} agent is $r_k \in \mathbb{C}$, while the velocity of the k^{th} agent is $\dot{r}_k = e^{i\theta_k} = \cos \theta_k + i \sin \theta_k$, where, $\theta_k \in S^1$ is the orientation of the (unit) velocity vector of the k^{th} agent from the real axis, and $i = \sqrt{-1}$ represents the standard complex number. The orientation θ_k of the velocity vector is also referred to as the phase of the k^{th} agent [20], [21]. In (1), $\omega_k \in \mathbb{R}$ is the angular frequency of the circular orbit performed by the k^{th} agent, which is determined by the feedback control $u_k \in \mathbb{R}$. If the control law u_k is constant and equal to $\omega_k \neq 0$, then the k^{th} agent travels at constant unit speed on a circle of radius $\rho_k = |\omega_k|^{-1}$. The direction of rotation around the circle is determined by the sign of ω_k . If $\omega_k > 0$, then the k^{th} agent rotates in the anticlockwise direction, whereas, if $\omega_k < 0$, then the k^{th} agent rotates in the clockwise direction.

Let the initial motion of all the agents with dynamics (1) be governed by the open-loop control $u_k = 0, \forall k$. In this situation, the k^{th} agent moves in a circular orbit at angular frequency ω_k . We seek a feedback control u_k such that the collective motion of agents, subjected to limited communication constraints represented by a time-invariant undirected graph, converge at desired angular frequency with their phase angles in synchronized and balanced states. Note that issues of collision avoidance among agents are not considered in this work.

B. Notations

We introduce some notations and state some important results here. We use bold face letters $\mathbf{r} = (r_1, \dots, r_N)^T \in \mathbb{C}^N$, $\boldsymbol{\theta} = (\theta_1, \dots, \theta_N)^T \in \mathbb{T}^N$, where, \mathbb{T}^N is the N -torus, which is equal to $S^1 \times \dots \times S^1$ (N -times), and $\boldsymbol{\omega} = (\omega_1, \dots, \omega_N)^T \in \mathbb{R}^N$, to represent the vectors of length N for the agents' positions, headings and angular frequencies, respectively. Also, vectors $e^{i\boldsymbol{\theta}}$ and $\mathbf{1}$ are used to represent by $e^{i\boldsymbol{\theta}} = (e^{i\theta_1}, \dots, e^{i\theta_N})^T \in \mathbb{C}^N$ and $\mathbf{1} = (1, 1, \dots, 1)^T \in \mathbb{R}^N$, respectively. Next, we define the inner product $\langle z_1, z_2 \rangle$ of two complex numbers $z_1, z_2 \in \mathbb{C}$ as $\langle z_1, z_2 \rangle = \text{Re}(\bar{z}_1 z_2)$, where \bar{z}_1 represents the complex conjugate of z_1 . For vectors, we use the analogous boldface notation $\langle \mathbf{w}, \mathbf{z} \rangle = \text{Re}(\mathbf{w}^* \mathbf{z})$ for $\mathbf{w}, \mathbf{z} \in \mathbb{C}^N$, where \mathbf{w}^* denotes the conjugate transpose of \mathbf{w} .

C. Representation of Limited Communication Constraints

In the framework of multiagent systems, communication among agents is described by means of a graph. A graph is a pair $G = (V, E)$, where $V = \{v_1, \dots, v_N\}$ is a set of N nodes or vertices and $E \subseteq V \times V$ is a set of edges or links. Elements of E are denoted as (v_j, v_k) which is termed an edge or a link from v_j to v_k , and is usually represented by an arrow with its tail at v_j and its head at v_k . If both links (v_j, v_k) and (v_k, v_j) belong to E then we combine these two links as one undirected link and use a bidirectional arrow to denote this link. An undirected link between nodes v_j and v_k indicates

that the information can be shared from node v_j to node v_k and vice versa. A graph G is called an undirected graph if it consists of only undirected links. Otherwise, the graph G is called a directed graph or digraph.

The node v_j is called a neighbor of node v_k if the link (v_j, v_k) exists in the graph G . It means that for directed graphs containing a link (v_j, v_k) , only the tail node v_j is a neighbor of the head node v_k and not vice versa. On the other hand, for undirected graphs, if node v_j is a neighbor of node v_k , then node v_k is also a neighbor of node v_j . In this paper, the set of neighbors of node v_j is represented by \mathcal{N}_j .

A directed path is a sequence of p nodes v_1, \dots, v_p , such that $(v_j, v_{j+1}) \in E, \forall j = 1, \dots, p-1$. A graph is called strongly connected if there exists a directed path from any one node to another. For an undirected graph, strong connectedness is simply called as connectedness. A complete graph is an undirected graph in which every pair of nodes is connected, that is, $(v_j, v_k) \in E, \forall j, k \in N$.

The Laplacian matrix of a graph G , denoted by $L = [l_{jk}] \in \mathbb{R}^{N \times N}$, is defined as [24],

$$l_{jk} = \begin{cases} |\mathcal{N}_j|, & \text{if } j = k \\ -1, & \text{if } k \in \mathcal{N}_j \\ 0 & \text{otherwise} \end{cases}$$

where, $|\mathcal{N}_j|$ is the cardinality of the set \mathcal{N}_j . This definition allows the representation of the several properties of a graph in the form of matrix properties of its Laplacian L . Some of the important properties of the Laplacian matrix which are relevant to this paper can be found in [2], and are as follows: (P1) The Laplacian matrix L of an undirected graph G is symmetric and positive semi-definite. (P2) If the graph G is strongly connected, then the Laplacian matrix L has an eigenvalue of zero associated with the eigenvector $\mathbf{1}$, that is, $L\mathbf{x} = 0$ iff $\mathbf{x} = \mathbf{1}x_0$.

In this paper, we will also use the notion of a circulant graph. A graph is circulant if and only if its Laplacian matrix L is a circulant matrix, that is, L is completely defined by its first row [25]. Each subsequent row of a circulant matrix is the previous row shifted one position to the right with the first entry of the row equal to the last entry of the previous row. An example of an undirected circulant graph, consisting of 6 nodes, is shown in Fig. 1. Note that the Laplacian matrices for the graphs in Figs. 1(a) and 1(b) are, respectively, given by $L_a = \text{circ}(1, 0, 0, -1, 0, 0)$ and $L_b = \text{circ}(2, -1, 0, 0, 0, -1)$, where, $\text{circ}(z)$ represents the circulant matrix with z being its first row. As both L_a and L_b are circulant matrices, both the graphs shown in Fig. 1 are circulant, but only the graph shown in Fig. 1(b) is connected.

III. DESIGN OF CONTROL LAWS

The design of control laws is described in this section. At first, a phase potential $W_L(\boldsymbol{\theta})$ is described, the minimization of which corresponds to synchronized formation, and its maximization corresponds to balanced formation. Then, a potential function $G(\boldsymbol{\omega})$ whose minimization leads to the desired angular frequency of all the agents, is proposed. Finally, the control law u_k is obtained by minimizing a composite Lyapunov function consisting of $W_L(\boldsymbol{\theta})$ and $G(\boldsymbol{\omega})$ as described below.

A. Achieving Synchronized and Balanced Formations

The average linear momentum of a group of agents plays an important role in stabilizing their synchronized and balanced formations. It is maximized in synchronized formation and minimized in balanced formation. From (1), the average linear momentum, p_θ , of a group of N -agents, is given by,

$$p_\theta = \frac{1}{N} \sum_{k=1}^N e^{i\theta_k}, \quad (2)$$

which is also referred to as the phase order parameter [23]. The phase arrangement $\boldsymbol{\theta}$ is synchronized if the modulus of the phase order parameter (2) equals one, that is, $|p_\theta| = 1$. The phase arrangement $\boldsymbol{\theta}$ is balanced if the phase order parameter (2) equals zero, that is, $p_\theta = 0$ [25].

Thus, the stabilization of synchronized and balanced formations is accomplished by considering the potential [1]

$$U(\boldsymbol{\theta}) = (N/2)|p_\theta|^2, \quad (3)$$

which reaches its unique minimum when $p_\theta = 0$ (balanced) and its unique maximum when all phases are identical (synchronized). All other critical points of $U(\boldsymbol{\theta})$ are isolated in the shape manifold \mathbb{T}^N/S^1 and are saddle points of $U(\boldsymbol{\theta})$ [1].

Based on this potential function, the design of control law for the all-to-all communication among agents may be accomplished [4]. However, in order to account for limited communication among agents, we modify the potential function (3) in the following manner [2].

Let $P = I_N - (1/N)\mathbf{1}\mathbf{1}^T$, where I_N is an $N \times N$ -identity matrix. Then, $Pe^{i\boldsymbol{\theta}} = e^{i\boldsymbol{\theta}} - p_\theta\mathbf{1}$. One can obtain the equality

$$\|p_\theta e^{i\boldsymbol{\theta}}\|^2 = \langle e^{i\boldsymbol{\theta}}, Pe^{i\boldsymbol{\theta}} \rangle = N(1 - |p_\theta|^2), \quad (4)$$

which is minimized in synchronized formation and maximized in balanced formation. Since, P is $(1/N)$ times the Laplacian matrix of the complete graph, the identity (4) suggests that the optimization of $U(\boldsymbol{\theta})$ in (3) may be replaced by the optimization of

$$W_L(\boldsymbol{\theta}) = Q_L(e^{i\boldsymbol{\theta}}) = (1/2) \langle e^{i\boldsymbol{\theta}}, Le^{i\boldsymbol{\theta}} \rangle, \quad (5)$$

which is a Laplacian quadratic form associated with L , and is positive semi-definite. Note that, for a connected graph, the quadratic form (5) vanishes only when $e^{i\boldsymbol{\theta}} = e^{i\theta_c}\mathbf{1}$, where $\theta_c \in S^1$ is a constant (see property P2), that is, the potential $W_L(\boldsymbol{\theta})$ is minimized in the synchronized formation.

The time derivative of $W_L(\boldsymbol{\theta})$, along the dynamics (1), is

$$\dot{W}_L(\boldsymbol{\theta}) = \sum_{k=1}^N \frac{\partial W_L}{\partial \theta_k} \dot{\theta}_k = \sum_{k=1}^N \frac{\partial W_L}{\partial \theta_k} \omega_k. \quad (6)$$

Note that

$$\frac{\partial W_L}{\partial \theta_k} = \frac{1}{2} \sum_{j=1}^N \frac{\partial}{\partial \theta_k} \langle e^{i\theta_j}, L_j e^{i\boldsymbol{\theta}} \rangle = \langle ie^{i\theta_k}, L_k e^{i\boldsymbol{\theta}} \rangle, \quad (7)$$

where, L_k is the k^{th} row of the Laplacian matrix L . Substituting (7) in (6), we get

$$\dot{W}_L(\boldsymbol{\theta}) = \sum_{k=1}^N \langle ie^{i\theta_k}, L_k e^{i\boldsymbol{\theta}} \rangle \omega_k. \quad (8)$$

Now, we state the following lemmas from [25], which describes various properties of the phase potential $W_L(\boldsymbol{\theta})$ that will be useful in proving the results in this paper.

Lemma 1: Let L be the Laplacian of an undirected and connected graph $G = (V, E)$. Consider the Laplacian phase potential $W_L(\boldsymbol{\theta})$ defined in (5). The potential $W_L(\boldsymbol{\theta})$ reaches its global minimum if and only if $\boldsymbol{\theta}$ is synchronized. If G is circulant, then $W_L(\boldsymbol{\theta})$ reaches its global maximum in a balanced phase arrangement.

Lemma 2: Let L be the Laplacian of a circulant and connected graph $G = (V, E)$, then the Laplacian phase potential $W_L(\boldsymbol{\theta})$, defined in (5), satisfies $0 \leq W_L(\boldsymbol{\theta}) \leq (N/2)\lambda_{\max}$, where $\lambda_{\max} > 0$ is the maximum eigenvalue of L .

B. Achieving Desired Angular Frequency

The agents, initially rotating at different angular frequencies, are required to stabilize their collective motion at desired angular frequency Ω_d (and hence achieve the desired radius $\rho_d = |\Omega_d|^{-1}$). For this, we choose a candidate Lyapunov function

$$G(\boldsymbol{\omega}) = \frac{1}{2} \sum_{k=1}^N (\omega_k - \Omega_d)^2 \quad (9)$$

which is minimized when $\omega_k = \Omega_d$, for all $k = 1, \dots, N$.

The time derivative of G , along the dynamics (1), yields

$$\dot{G}(\boldsymbol{\omega}) = \sum_{k=1}^N (\omega_k - \Omega_d) \dot{\omega}_k = \sum_{k=1}^N (\omega_k - \Omega_d) u_k \quad (10)$$

C. Composite Lyapunov Function and Control Law

In this subsection, the control law u_k is proposed by constructing a composite Lyapunov function, which ensures that all the agents travel around different circles at a desired angular frequency Ω_d with their phases either in balanced or in synchronized states.

Theorem 1: Consider system dynamics (1) with control law

$$u_k = -K \left((\omega_k - \Omega_d) - \left\langle i e^{i\theta_k}, L_k e^{i\boldsymbol{\theta}} \right\rangle \right) \quad (11)$$

where, L_k is the k^{th} row of the Laplacian L of an undirected and connected circulant graph $G = (V, E)$. For $K > 0$, all the agents converge to a collective motion in which they travel around different circles of the same radius $\rho_d = |\Omega_d|^{-1}$ with their relative phases in balanced state.

Proof: Consider a composite Lyapunov function

$$V_1(\boldsymbol{\theta}, \boldsymbol{\omega}) = K((N/2)\lambda_{\max} - W_L(\boldsymbol{\theta})) + G(\boldsymbol{\omega}); \quad K > 0 \quad (12)$$

Note that $0 \leq W_L(\boldsymbol{\theta}) \leq (N/2)\lambda_{\max}$ (see Lemma 2), which ensures that $\dot{V}_1 \geq 0$. Using (8) and (10), the time derivative of the Lyapunov function V_1 along the dynamics (1), is

$$\dot{V}_1(\boldsymbol{\theta}, \boldsymbol{\omega}) = -K \sum_{k=1}^N \left\langle i e^{i\theta_k}, L_k e^{i\boldsymbol{\theta}} \right\rangle \omega_k + \sum_{k=1}^N (\omega_k - \Omega_d) u_k \quad (13)$$

With the control law (11), the time derivative of V_1 results in

$$\dot{V}_1(\boldsymbol{\theta}, \boldsymbol{\omega}) = -K \sum_{k=1}^N (\omega_k - \Omega_d)^2 - K \Omega_d \sum_{k=1}^N \left\langle i e^{i\theta_k}, L_k e^{i\boldsymbol{\theta}} \right\rangle \quad (14)$$

Note that

$$\sum_{k=1}^N \left\langle i e^{i\theta_k}, L_k e^{i\boldsymbol{\theta}} \right\rangle = -\frac{1}{N} \sum_{k=1}^N \sum_{j \in \mathcal{N}_k} \sin(\theta_j - \theta_k) = 0 \quad (15)$$

Using (15), (14) becomes

$$\dot{V}_1(\boldsymbol{\theta}, \boldsymbol{\omega}) = -K \sum_{k=1}^N (\omega_k - \Omega_d)^2 \leq 0 \quad (16)$$

According to LaSalle's invariance theorem [26], all the solutions of (1) with the control law (11) converge to the largest invariant set in which $\dot{V}_1 = 0$, that is, the set contained in

$$\Lambda = \{ \boldsymbol{\omega} \mid \omega_k = \Omega_d, \forall k \}. \quad (17)$$

In Λ , $\omega_k = \Omega_d$ and $u_k = \dot{\omega}_k = 0$, $\forall k$, which implies that each agent rotates at angular frequency Ω_d . Moreover, $(N/2)\lambda_{\max} - W_L(\boldsymbol{\theta})$ also approaches zero due to the non-increasing nature of V_1 (since $\dot{V}_1 \leq 0$). As a result, the phase arrangement of the agents, in the set Λ , is given by the set of $\boldsymbol{\theta}$ where $W_L(\boldsymbol{\theta}) = (N/2)\lambda_{\max}$, that is, $W_L(\boldsymbol{\theta})$ attains its maximum value. It ensures phase balancing of $\boldsymbol{\theta}$ (see Lemma 1). ■

Theorem 2: Consider system dynamics (1) with control law

$$u_k = K \left((\omega_k - \Omega_d) + \left\langle i e^{i\theta_k}, L_k e^{i\boldsymbol{\theta}} \right\rangle \right) \quad (18)$$

where, L_k is the k^{th} row of the Laplacian L of an undirected and connected graph $G = (V, E)$. For $K < 0$, all the agents converge to a collective motion in which they travel around different circles of same radius $\rho_d = |\Omega_d|^{-1}$ with their relative phases in synchronized state.

Proof: Consider a composite Lyapunov function

$$V_2(\boldsymbol{\theta}, \boldsymbol{\omega}) = -K W_L(\boldsymbol{\theta}) + G(\boldsymbol{\omega}); \quad K < 0 \quad (19)$$

Using (8) and (10), the time derivative of the Lyapunov function V_2 along the dynamics (1), is

$$\dot{V}_2(\boldsymbol{\theta}, \boldsymbol{\omega}) = -K \sum_{k=1}^N \left\langle i e^{i\theta_k}, L_k e^{i\boldsymbol{\theta}} \right\rangle \omega_k + \sum_{k=1}^N (\omega_k - \Omega_d) u_k \quad (20)$$

With the control law (18), the time derivative of V_2 results in

$$\dot{V}_2(\boldsymbol{\theta}, \boldsymbol{\omega}) = K \sum_{k=1}^N (\omega_k - \Omega_d)^2 - K \Omega_d \sum_{k=1}^N \left\langle i e^{i\theta_k}, L_k e^{i\boldsymbol{\theta}} \right\rangle \quad (21)$$

Using (15), (21) becomes

$$\dot{V}_2(\boldsymbol{\theta}, \boldsymbol{\omega}) = K \sum_{k=1}^N (\omega_k - \Omega_d)^2 \leq 0. \quad (22)$$

According to LaSalle's invariance theorem [26], all the solutions of (1) with the control law (18) converge to the largest invariant set in which $\dot{V}_2 = 0$, that is, the set contained in Λ , defined by (17). In Λ , $\omega_k = \Omega_d$ and $u_k = \dot{\omega}_k = 0, \forall k$, which implies that each agent rotates at angular frequency Ω_d . Moreover, $W_L(\boldsymbol{\theta})$ also approaches zero due to the non-increasing nature of V_2 (since $\dot{V}_2 \leq 0$). As a result, the phase arrangement of the agents, in the set Λ , is given by the set of $\boldsymbol{\theta}$ where $W_L(\boldsymbol{\theta}) = 0$, that is, $W_L(\boldsymbol{\theta})$ attains its minimum value. It ensures phase synchronization of $\boldsymbol{\theta}$ (see Lemma 1). ■

Example 1: In this example, Theorems 1 and 2 are demonstrated through simulation of $N = 6$ agents connected via a graph as shown in Fig. 1(b). Let the initial positions, initial heading angles and initial angular frequencies of the agents be $\mathbf{r}(0) = ((1, -1), (10, 3), (-1, -5), (-5, 1), (12, 5), (-4, 10))^T$, $\boldsymbol{\theta}(0) = (30^\circ, 45^\circ, 120^\circ, 75^\circ, 90^\circ, 60^\circ)^T$, and $\boldsymbol{\omega}(0) = (0.2, -0.3, 0.4, -0.5, 0.6, -0.8)^T$, respectively.

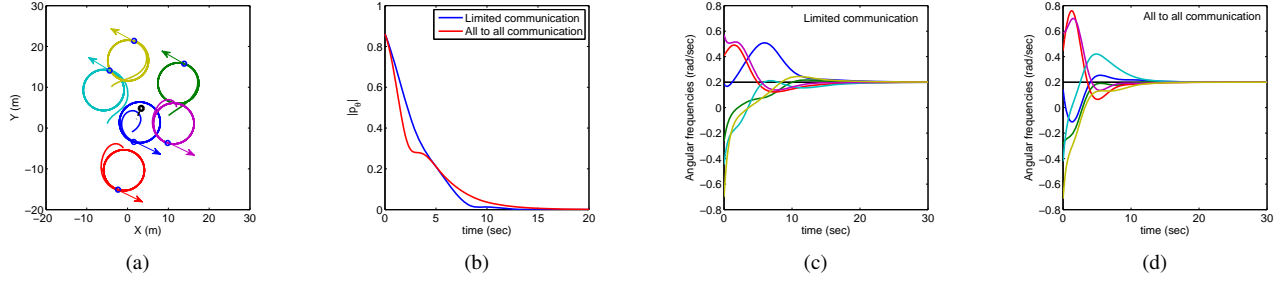


Fig. 2. Balancing of $N = 6$ agents, connected by a graph as shown in Fig.1(b), on different circles, each having the desired radius $\rho_d = |\Omega_d|^{-1} = 5$ m. (a) Trajectories of the agents under the control laws (11) with $K = 1$. (b) Average linear momentum approaches zero with time. (c) Consensus of angular frequencies at desired value $\Omega_d = 0.2$ rad/sec (limited communication case). (d) Consensus of angular frequencies at desired value $\Omega_d = 0.2$ rad/sec (all-to-all communication case)

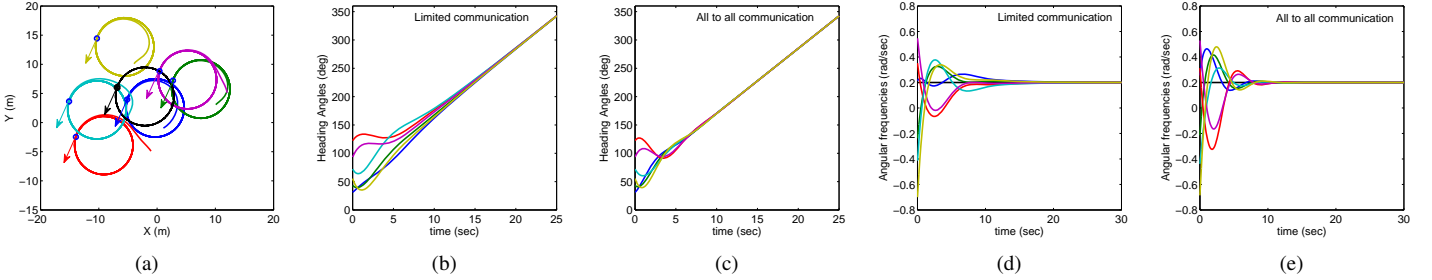


Fig. 3. Synchronization of $N = 6$ agents, connected by a graph as shown in Fig.1(b), on different circles, each having the desired radius $\rho_d = |\Omega_d|^{-1} = 5$ m. (a) Trajectories of the agents under the control laws (18) with $K = -1$. (b) Consensus in heading angles (limited communication case). (c) Consensus in heading angles (all-to-all communication case). (d) Consensus of angular frequencies at desired value $\Omega_d = 0.2$ rad/sec (limited communication case). (e) Consensus of angular frequencies at desired value $\Omega_d = 0.2$ rad/sec (all-to-all communication case). Since the agents continue to rotate around their respective circles in synchronized fashion, their heading angles keep increasing with time.

Fig. 2 shows balancing of the agents around different circles at desired angular frequency $\omega_d = 0.2$ rad/sec, and hence desired radius $\rho_d = |\Omega_d|^{-1} = 5$ m of circular orbits as expected. Fig. 3 shows synchronization on different circles at the same desired angular frequency and radius. In all figures in this paper, the trajectory of the centroid is shown in black. Note that, in these figures, the convergence of the angular frequencies to the desired value is faster under all-to-all communication scenario.

IV. MOTION ON A COMMON CIRCLE

In this section, we achieve synchronized and balanced formations of agents on a common circle of desired radius and fixed center, as shown in Fig. 4. The k^{th} agent rotates in the anticlockwise direction on a circle of radius $\rho_d = \Omega_d^{-1} > 0$ and center c_d . Without loss of generality, we assume $\Omega_d > 0$. Therefore, at equilibrium, all the agents, which may initially be rotating in clockwise and anticlockwise directions, move in anticlockwise direction on a common circle of desired radius as well as center. The position r_k of the k -th agent in Fig. 4, is given by

$$r_k = c_d - i\rho_d e^{i\theta_k}. \quad (23)$$

To stabilize circular formation of all the agents around a common circle of radius $\rho_d = \Omega_d^{-1} > 0$ and center c_d , which is fixed, we introduce an error variable $e_k = r_k - (c_d -$

$i\rho_d e^{i\theta_k})$, $\forall k$, and choose a candidate Lyapunov function as,

$$\begin{aligned} S(\mathbf{r}, \boldsymbol{\theta}) &= \frac{1}{2} \sum_{k=1}^N |e_k|^2 = \frac{1}{2} \sum_{k=1}^N |r_k - c_d + i\rho_d e^{i\theta_k}|^2 \\ &= \frac{1}{2} \sum_{k=1}^N \langle r_k - c_d + i\rho_d e^{i\theta_k}, r_k - c_d + i\rho_d e^{i\theta_k} \rangle \end{aligned} \quad (24)$$

which is a positive-definite function and approaches zero when $r_k = c_d - i\rho_d e^{i\theta_k}$, $\forall k$. It means that the minimization of $S(\mathbf{r}, \boldsymbol{\theta})$ corresponds to the situation when all the agents of the group move on a common circle of radius ρ_d centered at the fixed point c_d .

The time derivative of the Lyapunov function (24) along the dynamics (1), yields

$$\dot{S}(\mathbf{r}, \boldsymbol{\theta}) = \sum_{k=1}^N \langle r_k - c_d - i\rho_d e^{i\theta_k}, e^{i\theta_k} (1 - \rho_d \omega_k) \rangle \quad (25)$$

Using linearity of inner product [22] in (25), we get

$$\begin{aligned} \dot{S}(\mathbf{r}, \boldsymbol{\theta}) &= \sum_{k=1}^N \langle r_k - c_d, e^{i\theta_k} \rangle (1 - \rho_d \omega_k) \\ &\quad - \sum_{k=1}^N \rho_d \langle i e^{i\theta_k}, e^{i\theta_k} \rangle (1 - \rho_d \omega_k) \end{aligned} \quad (26)$$

Since $\langle i e^{i\theta_k}, e^{i\theta_k} \rangle = 0$, (26) is simplified to

$$\dot{S}(\mathbf{r}, \boldsymbol{\theta}) = \sum_{k=1}^N \langle r_k - c_d, e^{i\theta_k} \rangle (1 - \rho_d \omega_k). \quad (27)$$

Theorem 3: Consider system dynamics (1) with control law

$$u_k = -\kappa\rho_d(\omega_k - \Omega_d) + \Omega_d^2 \left(\kappa \langle r_k - c_d, e^{i\theta_k} \rangle + K \langle ie^{i\theta_k}, L_k e^{i\theta} \rangle \right), \quad (28)$$

where, L_k is the k^{th} row of the Laplacian L of an undirected and connected circulant graph $G = (V, E)$. For $K > 0$ and $\kappa > 0$, all the agents converge to a circular formation in which they travel around a common circle of radius $\rho_d = \Omega_d^{-1} > 0$ and center c_d in the anticlockwise direction with their relative phases in the balanced state.

Proof: Consider a composite Lyapunov function

$$U_1(\mathbf{r}, \boldsymbol{\theta}, \boldsymbol{\omega}) = \kappa S(\mathbf{r}, \boldsymbol{\theta}) + \rho_d K ((N/2)\lambda_{\max} - W_L(\boldsymbol{\theta})) + \rho_d^3 G(\boldsymbol{\omega}). \quad (29)$$

Using (8), (10) and (27), the time derivative of the Lyapunov function U_1 along the dynamics (1), is

$$\begin{aligned} \dot{U}_1(\mathbf{r}, \boldsymbol{\theta}, \boldsymbol{\omega}) &= \kappa \sum_{k=1}^N \langle r_k - c_d, e^{i\theta_k} \rangle (1 - \rho_d \omega_k) \\ &+ K \sum_{k=1}^N \langle ie^{i\theta_k}, L_k e^{i\theta} \rangle (-\rho_d \omega_k) + \rho_d^3 \sum_{k=1}^N (\omega_k - \Omega_d) u_k \end{aligned} \quad (30)$$

Using (15), (30) can be rewritten as

$$\begin{aligned} \dot{U}_1(\mathbf{r}, \boldsymbol{\theta}, \boldsymbol{\omega}) &= \sum_{k=1}^N \left(\kappa \langle r_k - c_d, e^{i\theta_k} \rangle + K \langle ie^{i\theta_k}, L_k e^{i\theta} \rangle \right) \\ &\times (1 - \rho_d \omega_k) + \rho_d^3 \sum_{k=1}^N (\omega_k - \Omega_d) u_k \end{aligned} \quad (31)$$

Under control law (28), the time derivative of U_1 results in

$$\dot{U}_1(\mathbf{r}, \boldsymbol{\theta}, \boldsymbol{\omega}) = -\kappa\rho_d^4 \sum_{k=1}^N (\omega_k - \Omega_d)^2 \leq d \quad (32)$$

According to LaSalle's invariance principle [26], all the solutions of (1) with the control law (28) converge to the largest invariant set in which $\dot{U}_1 = 0$, that is, the set contained in Λ defined by (17). In Λ , $\omega_k = \Omega_d$ and $\dot{\omega}_k = d, \forall k$, which implies that

$$\kappa \langle r_k - c_0, e^{i\theta_k} \rangle + K \langle ie^{i\theta_k}, L_k e^{i\theta} \rangle = 0, \quad \forall k. \quad (33)$$

Also, in the set Λ , second eq. of dynamics (1) reduces to

$$\dot{\theta}_k = \Omega_d \quad (34)$$

which, upon integration, yields

$$\theta_k(t) = \Omega_d t + \theta_k(0) = \phi_k(t) \text{ (say)}. \quad (35)$$

Using (35), first eq. of dynamics (1) results in

$$\dot{r}_k = e^{i\phi_k(t)} \quad (36)$$

which, upon integration, yields

$$r_k(t) = r_k(0) - i\rho_d e^{i\phi_k(t)} \quad (37)$$

Here, $r_k(0)$ and $\theta_k(0)$ are constants. Now, we differentiate (33) with respect to time and obtain

$$\kappa \frac{d}{dt} \langle r_k - c_d, e^{i\theta_k} \rangle + K \frac{d}{dt} \langle ie^{i\theta_k}, L_k e^{i\theta} \rangle = 0 \quad (38)$$

Note that

$$\frac{d}{dt} \langle ie^{i\theta_k}, L_k e^{i\theta} \rangle = \langle -\Omega_d e^{i\theta_k}, L_k e^{i\theta} \rangle + \langle ie^{i\theta_k}, -i\Omega_d L_k e^{i\theta} \rangle = 0 \quad (39)$$

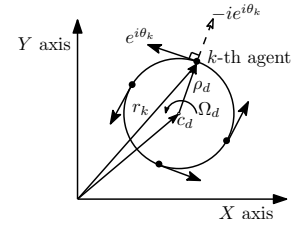


Fig. 4. Orientation of the k -th agent on a circle of desired radius $\rho_d = \Omega_d^{-1} > 0$ and center c_d .

Substituting (35), (37) and (39) in (38), we get

$$\frac{d}{dt} \langle r_k(0) - i\rho_d e^{i\phi_k(t)} - c_d, e^{i\phi_k(t)} \rangle = 0 \quad (40)$$

Using linearity of inner product [22] along with the fact that $\langle i\rho_d e^{i\phi_k(t)}, e^{i\phi_k(t)} \rangle = 0$, (40) simplifies to

$$\frac{d}{dt} \langle r_k(0) - c_d, e^{i\phi_k(t)} \rangle = 0 \quad (41)$$

Since, $r_k(0)$ and c_0 , both are constants. Therefore, (41) is satisfied only if

$$r_k(0) = c_d, \quad \forall k. \quad (42)$$

Substituting (42) in (37), yields

$$r_k(t) = c_d - i\rho_d e^{i\phi_k(t)}, \quad \forall k, \quad (43)$$

which is the position of the k^{th} agent rotating around a circle of radius ρ_d and center at c_d (see Eq. (23)). This implies that all the agents converge to a circular formation with radius $\rho_d = \Omega_d^{-1}$ and center c_d for $\kappa > 0$ and $K > 0$. Moreover, $(N/2)\lambda_{\max} - W_L(\boldsymbol{\theta})$ also approaches zero due to the non-increasing nature of U_1 (since $\dot{U}_1 \leq 0$). As a result, the phase arrangement of the agents, in the set Λ , is given by the set of $\boldsymbol{\theta}$ where $W_L(\boldsymbol{\theta}) = (N/2)\lambda_{\max}$, that is, $W_L(\boldsymbol{\theta})$ attains its maximum value. It ensures phase balancing of $\boldsymbol{\theta}$ (see Lemma 2). ■

Theorem 4: Consider system dynamics (1) with control law (28), where L_k is the k^{th} row of the Laplacian L of an undirected and connected graph $G = (V, E)$. For $K < 0$ and $\kappa > 0$, all the agents converge to a circular formation in which they move on a common circle of radius $\rho_d = \Omega_d^{-1} > 0$ and center c_d in anticlockwise direction with their relative phases in synchronized state.

Proof: Consider a composite Lyapunov function

$$U_2(\mathbf{r}, \boldsymbol{\theta}, \boldsymbol{\omega}) = \kappa S(\mathbf{r}, \boldsymbol{\theta}) - \rho_d K W_L(\boldsymbol{\theta}) + \rho_d^3 G(\boldsymbol{\omega}). \quad (44)$$

The time derivative of U_2 along the dynamics (1), yields

$$\dot{U}_2(\mathbf{r}, \boldsymbol{\theta}, \boldsymbol{\omega}) = \dot{U}_1 = -\kappa\rho_d^4 \sum_{k=1}^N (\omega_k - \Omega_d)^2 \leq 0. \quad (45)$$

Since $\dot{U}_2 = \dot{U}_1$, the proof follows the same steps as used to prove Theorem 3. This concludes that, $\forall k$, the circular formation with radius $\rho_d = \Omega_d^{-1}$ and center c_d is obtained for $\kappa > 0, K < 0$. Moreover, the potential $W_L(\boldsymbol{\theta})$ also approaches zero due to the non-increasing nature of U_2 (since $\dot{U}_2 \leq 0$). As a result, the phase arrangement of the agents, in the set Λ , is given by the set of $\boldsymbol{\theta}$ where $W_L(\boldsymbol{\theta}) = 0$, that is, $W_L(\boldsymbol{\theta})$ attains its minimum value. It ensures phase synchronization of $\boldsymbol{\theta}$ (see Lemma 1). This completes the proof. ■

Example 2: In this example, the simulation results are presented for the same 6 agents as considered in Example 1. Fig. 5

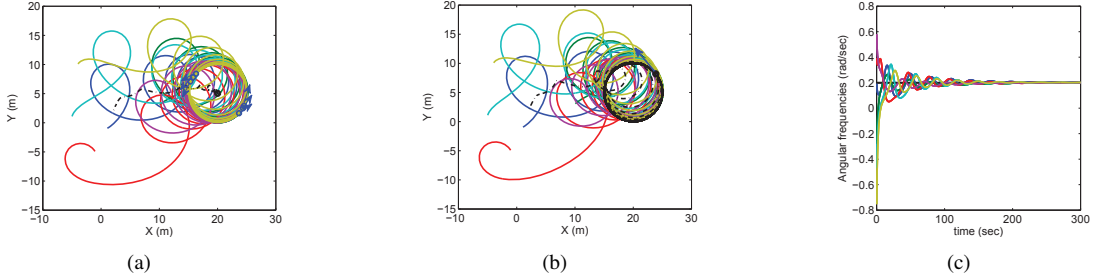


Fig. 5. Synchronization and balancing of $N = 6$ agents, connected by a graph as shown in Fig.1(b), around the common circle of desired radius $\rho_d = |\Omega_d|^{-1} = 5$ m and desired center $c_d = (20, 5)$. (a) Balanced formation under the control law (28) with $K = 0.5$ and $\kappa = 0.1$. (b) Synchronized formation under the control law (28) with $K = -1$ and $\kappa = 0.1$. (c) Consensus of angular frequencies at desired value $\Omega_d = 0.2$ rad/sec for balanced formation.

depicts the synchronization and balancing of the agents around a common circle at desired angular frequency $\Omega_d = 0.2$ rad/sec and desired center $c_0 = (20, 5)$. Balanced formation is shown in Fig. 5(a), and synchronized formation is shown in Fig. 5(b). In Fig. 5(c), the convergence of different angular frequencies of the agents to a desired value $\Omega_d = 0.2$ rad/sec, is shown in balanced formation only since the plot for synchronized formation is similar.

It is worth noting that, in Fig. 5(a), the final position of the centroid of the group coincides with the center $c_0 = (20, 5)$ of the common circle. This is due to the fact that, in balanced formation, the linear momentum $p_\theta = 0$, which causes (23) to reduce to $c_0 = (1/N) \sum_{k=1}^N r_k$ when summed over all k on both the sides, which is the average position of all the agents, or the position of their centroid.

V. SYMMETRIC BALANCED PATTERNS AROUND THE COMMON CIRCLE

In this section, we aim to achieve symmetric balanced patterns of the agents around a desired common circle, as in [1], [2] and [25], in which the agents are in balanced formation with a symmetrical arrangement of their phases.

Let $1 \leq M \leq N$ be a divisor of N . A symmetric arrangement of N phases consisting of M clusters uniformly spaced around the common circle, each with N/M synchronized phases, is called an (M, N) -pattern. For instance, the $(1, N)$ -pattern corresponds to the synchronized state and the (N, N) -pattern corresponds to the so-called splay state, which is characterized by N phases uniformly spaced around the common circle.

The m^{th} harmonic of the potential $W_L(\theta)$, which plays an important role in stabilizing symmetric phase patterns, is defined as

$$W_L^m(\theta) = \frac{1}{2} \langle e^{im\theta}, L e^{im\theta} \rangle, \quad (46)$$

where, $m \in \mathbb{N} \triangleq \{1, 2, 3, \dots\}$. Note that $W_L^m(\theta)$ is a natural generalization of the potential $W_L(\theta)$, which depends on the m^{th} phase vector $e^{im\theta}$. See [2] or [25] for a more detailed description.

We now state the following lemmas from [2] and [25] that are useful in proving the results of this section.

Lemma 3: If L is the Laplacian of a connected and balanced graph, then the global minimum of $W_L^m(\theta)$ is synchronized modulo $2\pi/m$, that is, $e^{im\theta} = e^{i\theta_0} \mathbf{1}_N$, where $\theta_0 \in S^1$. If the graph is circulant, then the global maximum of $W_L^m(\theta)$ is balanced modulo $2\pi/m$, that is, $\mathbf{1}^T e^{im\theta} = 0$.

Lemma 4: Let L be the Laplacian of a circulant and connected graph $G = (V, E)$, then the Laplacian phase potential

$W_L^m(\theta)$ defined in (46) satisfies $0 \leq W_L^m(\theta) \leq (N/2)\lambda_{\max}$, where $\lambda_{\max} > 0$ is the maximum eigenvalue of L .

Lemma 5: Let $1 \leq M \leq N$ be a divisor of N . An arrangement θ of N phases is an (M, N) -pattern if and only if, for all $m \in \{1, \dots, M-1\}$, the phase arrangement $m\theta$ is balanced and the phase arrangement $M\theta$ is synchronized.

Following Lemma 5, we choose a Laplacian based (M, N) potential function as

$$W_L^{M,N}(\theta) = \sum_{m=1}^{M-1} \frac{K_m}{m^2} \left(\frac{N}{2} \lambda_{\max} - W_L^m(\theta) \right) - \frac{K_M}{M^2} W_L^M(\theta), \quad (47)$$

with $K_m > 0$ for $m = 1, \dots, M-1$ and $K_M < 0$, which is minimized when $\theta, 2\theta, \dots, (M-1)\theta$ are balanced and $M\theta$ is synchronized, that is, the minimization of (47) gives rise to an (M, N) -pattern.

Substituting for $W_L^m(\theta)$ from (46) into (47), yields

$$W_L^{M,N}(\theta) = \frac{1}{2} \sum_{m=1}^{M-1} \frac{K_m}{m^2} \left(N \lambda_{\max} - \langle e^{im\theta}, L e^{im\theta} \rangle \right) - \frac{K_M}{2M^2} \langle e^{iM\theta}, L e^{iM\theta} \rangle, \quad (48)$$

whose time derivative along the dynamics (1), is given by

$$\dot{W}_L^{M,N}(\theta) = - \sum_{k=1}^N \sum_{m=1}^M K_m \langle i e^{im\theta_k}, L_k e^{im\theta} \rangle \omega_k. \quad (49)$$

Theorem 5: Consider system dynamics (1) with control law

$$u_k = -\kappa \rho_d (\omega_k - \Omega_d) + \Omega_d^2 \left(\kappa \langle r_k - c_d, e^{i\theta_k} \rangle + K \sum_{m=1}^M K_m \langle i e^{im\theta_k}, L_k e^{im\theta} \rangle \right) \quad (50)$$

where, L_k is the k^{th} row of the Laplacian L of an undirected and connected circulant graph $G = (V, E)$. For $K > 0$ and $\kappa > 0$, all the agents converge to a circular formation in which they travel around a common circle of radius $\rho_d = \Omega_d^{-1} > 0$ and center c_d in the anticlockwise direction with their relative phases in the (M, N) -pattern.

Proof: Consider a composite Lyapunov function

$$V(\mathbf{r}, \theta, \omega) = \kappa S(\mathbf{r}, \theta) + \rho_d K W_L^{M,N}(\theta) + \rho_d^3 G(\omega). \quad (51)$$

As $0 \leq W_L^m(\theta) \leq (N/2)\lambda_{\max}$ (see Lemma 4), it ensures that $W_L^{M,N}(\theta) \geq 0$. Using (10), (27) and (49), the time derivative

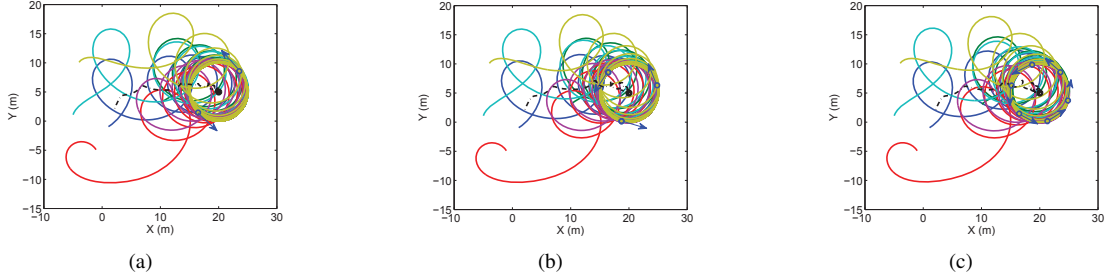


Fig. 6. Different symmetric balanced patterns of 6 agents, connected by a graph as shown in Fig.1(b), around the common circle of desired radius $\rho_d = |\Omega_d|^{-1} = 5$ m and desired center $c_0 = (20, 5)$, under the control law (50) with $K = 1, \kappa = K_m = 0.1$, and $K_M = -0.5$. (a) (2,6) pattern. (b) (3,6) pattern. (c) (6,6) pattern: splay formation.

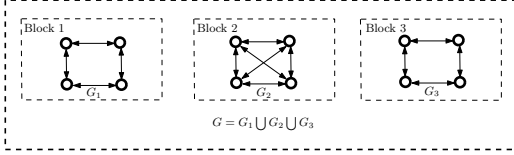


Fig. 7. Block interaction of 12 agents with 3 blocks, each containing 4 agents.

of the Lyapunov function V along the dynamics (1), is

$$\begin{aligned} \dot{V}(\mathbf{r}, \boldsymbol{\theta}, \boldsymbol{\omega}) &= \kappa \sum_{k=1}^N \left\langle r_k - c_d, e^{i\theta_k} \right\rangle (1 - \rho_d \omega_k) \\ &+ K \sum_{m=1}^M \sum_{k=1}^N K_m \left\langle i e^{im\theta}, L_k e^{im\theta} \right\rangle (-\rho_d \omega_k) + \rho_d^3 \sum_{k=1}^N (\omega_k - \Omega_d) u_k. \end{aligned} \quad (52)$$

Note that

$$\sum_{k=1}^N \left\langle i e^{im\theta_k}, L_k e^{im\theta} \right\rangle = -\frac{1}{N} \sum_{k=1}^N \sum_{j \in \mathcal{N}_k} \sin(m(\theta_j - \theta_k)) = 0 \quad (53)$$

Using (53), (52) can be rewritten as

$$\begin{aligned} \dot{V}(\mathbf{r}, \boldsymbol{\theta}, \boldsymbol{\omega}) &= \sum_{k=1}^N \left(\kappa \left\langle r_k - c_d, e^{i\theta_k} \right\rangle + K \sum_{m=1}^M K_m \left\langle i e^{im\theta}, L_k e^{im\theta} \right\rangle \right) \\ &\times (1 - \rho_d \omega_k) + \rho_d^3 \sum_{k=1}^N (\omega_k - \Omega_d) u_k. \end{aligned} \quad (54)$$

Under the control law (50), the time derivative of V results in

$$\dot{V}(\mathbf{r}, \boldsymbol{\theta}, \boldsymbol{\omega}) = \dot{U}_1 = -\kappa \rho_d^4 \sum_{k=1}^N (\omega_k - \Omega_d)^2 \leq 0. \quad (55)$$

Since $\dot{V} = \dot{U}_1$, the proof follows the same steps as in Theorem 3. Thus, $\forall k$, the circular formation with radius $\rho_d = |\Omega_d|^{-1}$ and center c_d is obtained for $K > 0$ and $\kappa > 0$. Moreover, the potential $W_L^{M,N}(\boldsymbol{\theta})$ is also minimized due to the non-increasing nature of V (since $\dot{V} \leq 0$). As a result, the phase arrangement of the agents, in the set Λ , is given by the set of $\boldsymbol{\theta}$ where $\boldsymbol{\theta} \in \mathbb{T}^N$ is an (M, N) -pattern. ■

Example 3: In this example, the simulation results are presented for the 6 agents considered in Example 1. Fig. 6 shows the different symmetric balanced patterns of the agents around the common circle of desired radius $\rho_d = |\Omega_d|^{-1} = 5$ m and center $c_0 = (20, 5)$. The arrangement in Fig. 6(c) is the splay state, in which the 6 agents are at equal angular

separation of 60° , as expected.

VI. ACHIEVING COORDINATED SUBGROUPS

Motivated by mobile sensor network applications, as discussed in [2], in this section, we propose control laws to stabilize multi-level configurations of a group of agents. A multi-level configuration is an arrangement of agents in subgroups around different circles in a symmetric pattern of their phase angles. In order to achieve these configurations, we divide the group of N agents into B blocks (subgroups) and refer to each block by its block index $b = 1, \dots, B$. For the sake of convenience, we assume that there is no interaction between subgroups unless specifically mentioned. Let the graph G_b describe the interaction between all the agents in block b . Collectively, the set of all interaction is defined by the graph $G \triangleq \bigcup_{b=1}^B G_b$. Note that the Laplacian matrix \hat{L} corresponding to graph G is a block-diagonal matrix, each block of which represents the Laplacian matrix of the graph G_b . For instance, consider a group of 12 agents divided into 3 blocks containing 4 agents in each block. Let their interaction network be represented by a graph $G = G_1 \cup G_2 \cup G_3$ as shown in Fig. 7. The Laplacian matrix corresponding to this block interaction is given by

$$\hat{L} = \begin{bmatrix} L_{G_1} & 0_{4 \times 4} & 0_{4 \times 4} \\ 0_{4 \times 4} & L_{G_2} & 0_{4 \times 4} \\ 0_{4 \times 4} & 0_{4 \times 4} & L_{G_3} \end{bmatrix} \quad (56)$$

where, $0_{4 \times 4}$ represents a 4×4 zero matrix, and $L_{G_1} = L_{G_3} = \text{circ}(2, -1, 0, -1)$ and $L_{G_2} = \text{circ}(3, -1, -1, -1)$ are the Laplacian matrices of the subgraphs $G_1 (= G_3)$ and G_2 , respectively. Since \hat{L} is a block diagonal matrix, its eigenvalues are the union of the eigenvalues of all block diagonal matrices [22].

We further assume that each agent is assigned to one and only one block, so that $\sum_{b=1}^B N_b = N$, where N_b is the number of agents in block b . Also, let $F^b = \{f_1^b, \dots, f_{N_b}^b\}$ be the set of agent indices, and $\rho_d^b = \{|\Omega_d^b|\}^{-1} > 0$ and c_d^b , respectively, be the radius, and center of the circle corresponding to the b -th block.

Based on these notations, the following corollaries to Theorems 3, 4 and 5 are now stated below.

Corollary 1: For $k \in F^b$, consider system dynamics (1) with control law

$$u_k = -\kappa \rho_d^b (\omega_k - \Omega_d^b) + \left\{ \Omega_d^b \right\}^2 \left(\kappa \left\langle r_k - c_d^b, e^{i\theta_k} \right\rangle + K \left\langle i e^{i\theta_k}, \hat{L}_k e^{i\theta} \right\rangle \right), \quad (57)$$

where, \hat{L}_k is the k^{th} row of the Laplacian \hat{L} of a graph $G = \bigcup_{b=1}^B G_b$ with G_b being an undirected and connected circulant

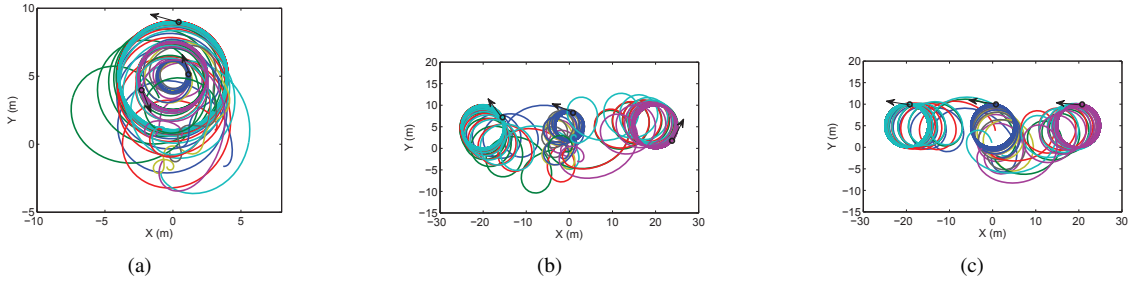


Fig. 8. Synchronization of 12 agents in 3 different groups, with 4 agents in each group, under the control law (57) with $K = -1$ and $\kappa = 0.5$. Synchronization on different circles with (a) different desired radius and the same desired center when the agents interact only within groups. (b) Different desired radius and centers when the agents interact only within groups. (c) Same desired radius and different desired centers when the agents interact not only within groups but also between groups according to an all-to-all communication topology.

subgraph. For $K > 0$ and $\kappa > 0$, all the agents belonging to the block b converge to a circular formation in which they move on a circle of radius $\rho_d^b = \{\Omega_d^b\}^{-1} > 0$ and center c_d^b in the anticlockwise direction with their relative phases in the balanced state.

Proof: Consider a composite Lyapunov function

$$U_1^b(\mathbf{r}, \boldsymbol{\theta}, \boldsymbol{\omega}) = \kappa S^b(\mathbf{r}, \boldsymbol{\theta}) + \rho_d^b K \left((N/2) \lambda_{\max} - W_{\hat{L}}(\boldsymbol{\theta}) \right) + \left\{ \rho_d^b \right\}^3 G^b(\boldsymbol{\omega}); \quad \kappa > 0, K > 0, \quad (58)$$

where,

$$S^b(\mathbf{r}, \boldsymbol{\theta}) = \frac{1}{2} \sum_{k=1}^N \left\langle r_k - c_d^b + i \rho_0^b e^{i\theta_k}, r_k - c_d^b + i \rho_d^b e^{i\theta_k} \right\rangle, \\ G^b(\boldsymbol{\omega}) = \frac{1}{2} \sum_{k=1}^N \left(\omega_k - \Omega_d^b \right)^2,$$

and λ_{\max} is the maximum eigenvalue of \hat{L} . Note that (58) is a Lyapunov function only for the b^{th} block, and has a structure similar to (29). Therefore, the proof is similar to the proof of Theorem 3 and hence omitted. ■

Corollary 2: For $k \in F^b$, consider system dynamics (1) with control law (57), where \hat{L}_k is the k^{th} row of the Laplacian \hat{L} of a graph $G = \bigcup_{b=1}^B G_b$ with G_b being an undirected and connected subgraph. For $K < 0$ and $\kappa > 0$, all the agents belonging to the block b converge to a circular formation in which they travel around a circle of radius $\rho_d^b = \{\Omega_d^b\}^{-1} > 0$ and center c_d^b in the anticlockwise direction with their relative phases in the synchronized state.

Proof: Consider a composite Lyapunov function

$$U_2^b(\mathbf{r}, \boldsymbol{\theta}, \boldsymbol{\omega}) = \kappa S^b(\mathbf{r}, \boldsymbol{\theta}) - \rho_d^b K W_{\hat{L}}(\boldsymbol{\theta}) + \left\{ \rho_d^b \right\}^3 G^b(\boldsymbol{\omega}), \quad (59)$$

which is obtained by replacing L , Ω_d , ρ_d and c_d in (44) by \hat{L} , Ω_d^b , ρ_d^b and c_d^b , respectively. Since the structure of (59) is similar to (44), the proof is also similar to the proof of Theorem 4 and hence omitted. ■

Corollary 3: For $k \in F^b$, consider system dynamics (1) with control law

$$u_k = -\kappa \rho_d^b (\omega_k - \Omega_d^b) + \left\{ \Omega_d^b \right\}^2 \left(\kappa \left\langle r_k - c_d^b, e^{i\theta_k} \right\rangle + K \sum_{m_b=1}^{M_b} K_{m_b} \left\langle i e^{i m_b \theta_k}, \hat{L}_k e^{i m_b \theta} \right\rangle \right), \quad (60)$$

where, \hat{L}_k is the k^{th} row of the Laplacian \hat{L} of a graph $G = \bigcup_{b=1}^B G_b$ with G_b being an undirected and connected circulant

subgraph. For $K > 0$ and $\kappa > 0$, all the agents belonging to the block b converge to a circular formation in which they travel around a circle of radius $\rho_d^b = \{\Omega_d^b\}^{-1} > 0$ and center c_d^b in the anticlockwise direction with their relative phases in the (M_b, N_b) -pattern, where $1 \leq M_b \leq N_b$ is a divisor of N_b in the b^{th} block.

Proof: Consider a composite Lyapunov function

$$V^b(\mathbf{r}, \boldsymbol{\theta}, \boldsymbol{\omega}) = \kappa S^b(\mathbf{r}, \boldsymbol{\theta}) + \rho_d^b K W_{\hat{L}}^{M_b, N_b}(\boldsymbol{\theta}) + \left\{ \rho_d^b \right\}^3 G^b(\boldsymbol{\omega}), \quad (61)$$

where,

$$W_{\hat{L}}^{M_b, N_b}(\boldsymbol{\theta}) = \frac{1}{2} \sum_{m_b=1}^{M_b-1} \frac{K_{m_b}}{m_b^2} \left(N_b \lambda_{\max} - \left\langle e^{i m_b \boldsymbol{\theta}}, \hat{L} e^{i m_b \boldsymbol{\theta}} \right\rangle \right) - \frac{K_{M_b}}{2 M_b^2} \left\langle e^{i M_b \boldsymbol{\theta}}, \hat{L} e^{i M_b \boldsymbol{\theta}} \right\rangle. \quad (62)$$

Note that (61) can be obtained by replacing L , Ω_d , ρ_d and c_d in (51), respectively, by \hat{L} , Ω_d^b , ρ_d^b and c_d^b along with N , M and m replaced by N_b , M_b and m_b , respectively. Thus, the proof is similar to Theorem 5 and hence omitted. ■

Suppose the desired radius of the circle, corresponding to each block, is the same, that is, $\rho_d^b = \rho_d$ for all $b = 1, \dots, B$. In such a situation, by assuming that the agents within a block can also interact with the agents in other block, we can use various interaction networks (among agents) in a single control algorithm since the phase potentials corresponding to the different communication topologies can be combined to get a single potential function. For instance, consider a group of agents comprising two types of interactions networks whose corresponding Laplacian matrices are L and \hat{L} . Let L correspond to the all-to-all interaction and \hat{L} correspond to the block interaction among agents. With these interactions, the Lyapunov function in (59) becomes

$$\hat{U}_2^b(\mathbf{r}, \boldsymbol{\theta}, \boldsymbol{\omega}) = \kappa S^b(\mathbf{r}, \boldsymbol{\theta}) - \rho_d K (W_L(\boldsymbol{\theta}) + W_{\hat{L}}(\boldsymbol{\theta})) + \rho_d^3 G(\boldsymbol{\omega}), \quad (63)$$

which accounts for both the interaction networks. Note that, unlike previous case of the different radius of the circles associated with each block, here we can combine all the phase stabilizing potentials independently to get a single potential function since $\rho_d^b = \rho_d$ for all $b = 1, \dots, B$. As a result, multi-level configurations of all the agents with their phases, collectively in balanced, synchronized or in splay state, are obtained.

Example 4: In this example, simulation results are presented for $N = 12$ agents whose initial positions, initial heading

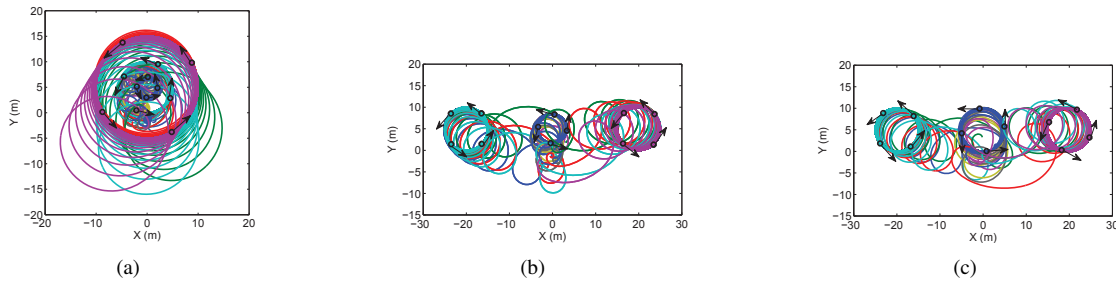


Fig. 9. Splay formation of 12 agents in 3 different groups, with 4 agents in each group, under the control law (60) with $K = 0.05$, $\kappa = 0.5$, $K_m = 10$, and $K_M = -0.5$. Splay formation on different circles with (a) Different desired radius and the same desired center when the agents interact only within groups. (b) Different desired radius and centers when the agents interact only within groups. (c) Same desired radius and centers when the agents interact not only within groups but also between groups according to an all-to-all communication topology.

angles and initial angular frequencies are randomly generated.

At first, we assume that the agents interact only in groups according to Fig. 7. In such a situation, synchronized and splay formations of the agents in three groups are shown in Figs. 8, and 9, respectively. The synchronized and splay formations of the agents, on the circles of different desired radius and the same desired center, are shown in Figs. 8(a) and 9(a), respectively, while the same, on the circles of different desired radius as well as centers is shown in Figs. 8(b) and 9(b), respectively.

Next, we assume that the agents interact in groups according to Fig. 7 as well as in subgroups according to an all-to-all communication topology. In this situation, the synchronized and splay formations of the agents, on the circles of the same desired radius and different desired centers, are shown in Figs. 8(c) and 9(c), respectively. Since the radius of all the circles corresponding to each group is same, the agents are collectively in synchronized and splay formations. In other words, if the heading phasors of all the agents were plotted on the same circle, then the resulting pattern would be synchronized or in splay state.

VII. CONCLUSIONS

This paper proposes a Laplacian-based control design methodology to stabilize synchronized and balanced collective motions of a group of agents either around different circles or around a common circle at a desired angular frequency under limited communication topology, which is represented by a time-invariant undirected graph. The feedback controls have been derived from composite Lyapunov functions, which reach their minimum in the desired configuration of the agents. From a practical point of view, various synchronized and balanced formations that are suitable for mobile sensors networks applications have been explored. Also, the class of collective motions studied in this paper, shows an interesting possibility for unmanned vehicles to expand and contract their formations about desired locations so as to better explore the search area.

REFERENCES

- [1] R. Sepulchre, D.A. Paley, and N.E. Leonard, "Stabilization of planar collective Motion: All-to-all communication," *IEEE Trans. Autom. Control*, vol. 52, no. 5, pp. 811-824, 2007.
- [2] R. Sepulchre, D.A. Paley, and N.E. Leonard, "Stabilization of planar collective motion with limited communication," *IEEE Trans. Autom. Control*, vol. 53, no. 3, pp. 706-719, 2008.
- [3] S. Napora, and D.A. Paley, "Observer-based feedback control for stabilization of collective motion," *IEEE Trans. Control Sys. Tech.*, vol. 21, no. 5, pp. 1846-1857, 2013.
- [4] A. Jain, and D. Ghose, "Stabilization of collective motion in synchronized, balanced and splay phase arrangements on a desired circle," *Proc. of the Amer. Control Conf.*, Chicago, IL, USA, pp. 731-736, July 2015.
- [5] A. Jain, and D. Ghose, "Collective behavior with heterogeneous controllers," *Proc. of the Amer. Control Conf.*, Washington, DC, USA, pp. 4636-4641, June 2013.
- [6] A. Jain, and D. Ghose, "Synchronization of multi-agent systems with heterogeneous controllers," *Submitted IEEE Trans. control Network Systems*.
- [7] A. Jain, and D. Ghose, "Achieving a desired collective centroid by a formation of agents moving in a controllable force field," *Accepted in Proc. of the Indian Control Conf.*, IIT Hyderabad, India, January 2016.
- [8] N. Ceccarelli, M.D. Marco, A. Garulli, and A. Giannitrapani, "Collective circular motion of multi-vehicle systems," *Automatica*, vol. 44, pp. 3025-3035, 2008.
- [9] G.S. Seyboth, J. Wu, J. Qin, C. Yu, and F. Allgöwer, "Collective circular motion of unicycle type vehicles with nonidentical constant velocities," *Trans. Control of Network Sys.*, vol. 1, no. 2, pp. 167-176, 2014.
- [10] L.B. Arranz, A. Seuret, and C.C. de Wit, "Translation control of a fleet circular formation of AUVs under finite communication range," *Proc. 48th IEEE Conf. on Dec. and Control*, Shanghai, China, pp. 8345-8350, December 2009.
- [11] L.B. Arranz, A. Seuret, and C.C. de Wit, "Contraction control of a fleet circular formation of AUVs under limited communication range," *Proc. Amer. Control Conf.*, Baltimore, MD, USA, pp. 5991-5996, 2010.
- [12] L.B. Arranz, A. Seuret, and C.C. de Wit, "Cooperative control design for time-varying formations of multi-agent systems," *IEEE Trans. Autom. Control*, vol. 59, no. 8, pp. 2283-2288, 2014.
- [13] Z. Chen, and H-T Zhang, "No-beacon collective circular motion of jointly connected multi-agents," *Automatica*, vol. 47, pp. 1929-1937, 2011.
- [14] Z. Chen, and H-T Zhang, "A remark on collective circular motion of heterogeneous multi-agents," *Automatica*, vol. 49, pp. 1236-1241, 2013.
- [15] J.A. Marshall, M.E. Broucke, and B.A. Francis, "Formations of vehicles in cyclic pursuit," *IEEE Tran. Autom. Control*, vol. 49, no. 11, pp. 1963-1974, 2004.
- [16] D.A. Paley, N.E. Leonard, and R. Sepulchre, "Oscillator models and collective motion: Splay state stabilization of self-propelled particles," *Proc. 44th IEEE Conf. on Dec. and Control*, Seville, Spain, pp. 3935-3940, December 2005.
- [17] J. Jeanne, N.E. Leonard, and D.A. Paley, "Collective motion of ring-coupled planar particles," *Proc. 44th IEEE Conf. on Dec. and Control*, Seville, Spain, pp. 3929-3934, December 2005.
- [18] J. Yu, S.M. LaValle, and D. Liberzon, "Rendezvous without coordinates," *IEEE Trans. Autom. Control*, vol. 57, no. 2, pp. 421434, 2012.
- [19] R. Zheng, and D. Sun, "Rendezvous of unicycles: A bearings-only and perimeter shortening approach," *Sys. Control Lett.*, vol. 62, no. 5, pp. 401-407, 2013.
- [20] D. Paley, and N.E. Leonard, and R. Sepulchre, "Collective motion and oscillator synchronization," *Proc. 2003 Block Island Workshop on Cooperative Control*, Springer-Verlag, pp. 189-205, Eds. 2004.
- [21] D.A. Paley, N.E. Leonard, R. Sepulchre, D. Grunbam, and J.K. Parrish, "Oscillator models and collective motion," *IEEE Control Sys. Magazine*, vol. 27, pp. 89-105, 2007.
- [22] C. Dorres and H. Anton, "Elementary Linear Algebra Applications version," 9th Ed., Wiley India Pvt. Ltd., 2011.
- [23] S.H. Strogatz, "From Kuramoto to Crawford: Exploring the onset of synchronization in populations of coupled oscillators," *Physica D: Nonlinear Phenomena*, 143(1-4), pp. 1-20, 2000.
- [24] H. Bai, M. Arcak, and J. Wen, "Cooperative Control Design: A Systematic, Passivity-based Approach," New York: Springer-Verlag, 2011.
- [25] D.A. Paley, "Cooperative control of collective motion for ocean sampling with autonomous vehicles," Ph.D. dissertation, The Department of Me-

- chanical and Aerospace Engineering, Princeton University, New Jersey, US, September 2007.
- [26] H. K. Khalil, "*Nonlinear Systems*," 3rd Ed., Upper Saddle River, NJ: Prentice-Hall, 2000.